

# Work functions and valence band states of pristine and Cs-intercalated single-walled carbon nanotube bundles

Satoru Suzuki<sup>a)</sup>

*NTT Basic Research Laboratories, Atsugi, Kanagawa, 243-0198 Japan*

Chris Bower

*Department of Physics and Astronomy, University of North Carolina at Chapel Hill, Chapel Hill, North Carolina 27599*

Yoshio Watanabe

*NTT Basic Research Laboratories, Atsugi, Kanagawa, 243-0198 Japan*

Otto Zhou

*Department of Physics and Astronomy, University of North Carolina at Chapel Hill, Chapel Hill, North Carolina 27599, and Curriculum in Applied and Materials Science, University of North Carolina at Chapel Hill, Chapel Hill, North Carolina 27599*

(Received 24 February 2000; accepted for publication 3 May 2000)

The electronic structures and the work functions of pristine and Cs-intercalated single-walled carbon nanotube bundles were investigated using ultraviolet photoemission spectroscopy. The valence bands of the pristine bundles were considerably altered from those of graphite. A spectral shift to the higher binding energy side was observed in the Cs-intercalated sample. The work function of the pristine bundles was found to be 4.8 eV, which is 0.1–0.2 eV larger than that of graphite. A drastic decrease of the work function to about 2.4 eV was observed in the Cs-intercalated sample. © 2000 American Institute of Physics. [S0003-6951(00)05326-2]

Recently, the investigation of the electronic properties of carbon nanotubes is becoming important in view of their potential applications in areas, such as electron field emission.<sup>1–3</sup> Experiments have shown that emitters made of single-walled carbon nanotubes (SWNTs) have low electron emission threshold field and high current capability compared with conventional emitters.<sup>3</sup> Although the low threshold field is generally attributed to the large field enhancement factor at the nanotube tip, precise understanding of the emission properties has been difficult due to uncertainty in the emitter geometry and the nanotube work function. Estimation of the work function based on the Fowler–Nordheim model<sup>4</sup> has suffered from the uncertainty of the local geometry.<sup>5</sup> Although carbon nanotubes have been investigated using various experimental techniques, only a few studies have used photoemission spectroscopy, which can provide the valence band electronic structure in a wide energy range. Moreover, photoemission spectroscopy has the advantage that it directly provides the work function without employing any uncertain parameters. Recently, Chen *et al.*<sup>6</sup> and Ago *et al.*<sup>7</sup> reported ultraviolet photoemission studies on multiwalled nanotubes (MWNTs). However, as far as we know, a corresponding investigation of the SWNTs is still lacking. In this letter, we applied ultraviolet photoemission spectroscopy (UPS) to investigate the electronic structures of pristine and Cs-intercalated SWNTs, and their work functions, which are crucial to understanding the field emission properties.

The SWNT bundles were synthesized by the laser ablation method.<sup>8</sup> The raw material was purified by ultrasonic-

assisted filtration and was then deposited on doped GaAs substrates by a spray method.<sup>9</sup> The thickness of the SWNT film was estimated to be 0.5  $\mu\text{m}$ . Transmission electron microscopy measurements<sup>9</sup> indicated the purified material contained mostly SWNT bundles. The average diameter of the nanotubes and bundles were evaluated to be 1.4 and 20 nm, respectively, by x-ray diffraction intensity simulation.<sup>10</sup> From a nuclear magnetic resonance (NMR) measurement,<sup>11</sup> the ratio of metallic and semiconducting tubes was estimated to be 1:2, suggesting a random helicity distribution.

Photoemission measurements were carried out at room temperature using an He discharge lamp (He I:  $h\nu = 21.22$  eV) and an angle-integrated-type electron energy analyzer. The base pressure of the analysis chamber was  $2 \times 10^{-9}$  Torr. The sample was biased by about  $-9$  V during the work function measurements to accelerate the low energy secondary electrons. The position of the Fermi level was calibrated by measuring the Fermi edge of an evaporated gold film. The typical probing depth of the UPS measurement was estimated to be a few nm. Thus, before the measurements, the pristine SWNT sample was annealed at 500 °C in a vacuum to remove adsorbates on the surface. The Cs-intercalated sample was prepared by depositing Cs atoms on the pristine sample at room temperature using an alkali-metal dispenser. Our previous studies<sup>8,12</sup> using an analytical electron microscope revealed that the alkali-metal atoms deposited on SWNT bundles intercalate into the bundles.

Figure 1 shows the valence band spectra of the pristine SWNTs and graphite. The prominent features of graphite observed at about 3, 5, and 8.2 eV can be identified as the  $\pi$  band, the top of the  $\sigma$ band +  $\pi$ band, and the bottom of the  $\pi$ band +  $\sigma$ band, respectively, by referring to a previous study.<sup>13</sup> According to the previous UPS study,<sup>6</sup> the spectrum

<sup>a)</sup>Electronic mail: ssuzuki@will.brl.ntt.co.jp

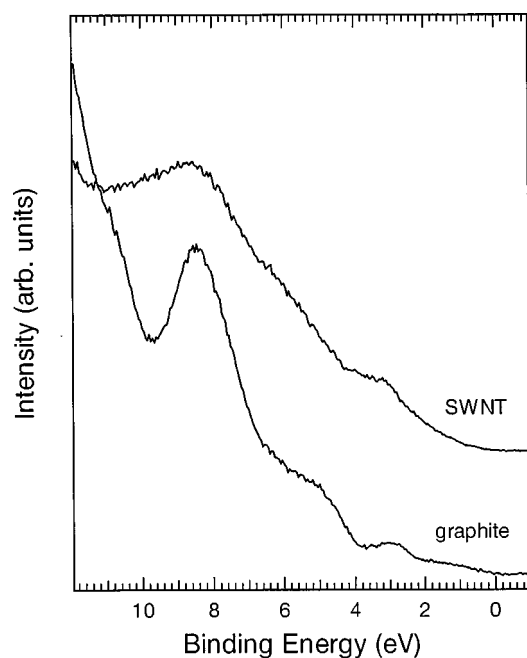


FIG. 1. Valence band photoemission spectra of the pristine SWNT bundles and graphite.

of MWNTs with diameters of 15–20 nm is very similar to that of graphite. In contrast, the spectra of the SWNT (diameter: 1.4 nm) bundles and graphite are considerably different, although the three corresponding features are also visible in the spectrum of the SWNTs. The electronic structural difference between the SWNTs and MWNTs originates mainly in the difference in the tube diameters rather than in the graphene sheet numbers. This is because the density of states of a MWNT can be roughly understood in terms of a superposition of that of individual nanotubes due to a weak inter-layer interaction.

The variation of the valence band spectrum caused by

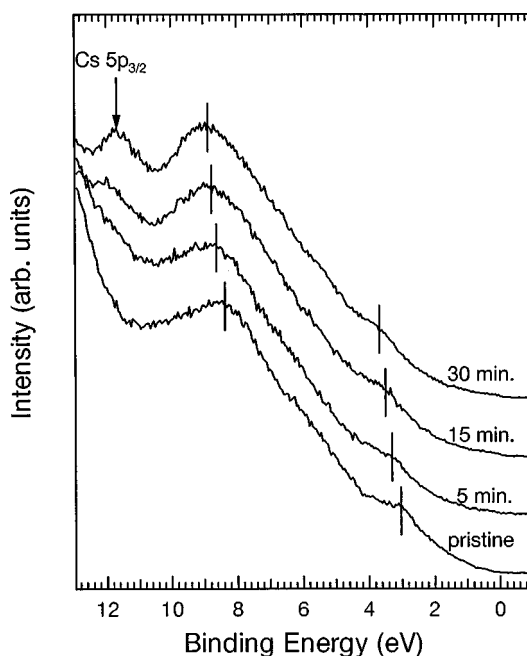


FIG. 2. Valence band photoemission spectra of the pristine and Cs-intercalated SWNT bundles. The Cs deposition times are denoted.

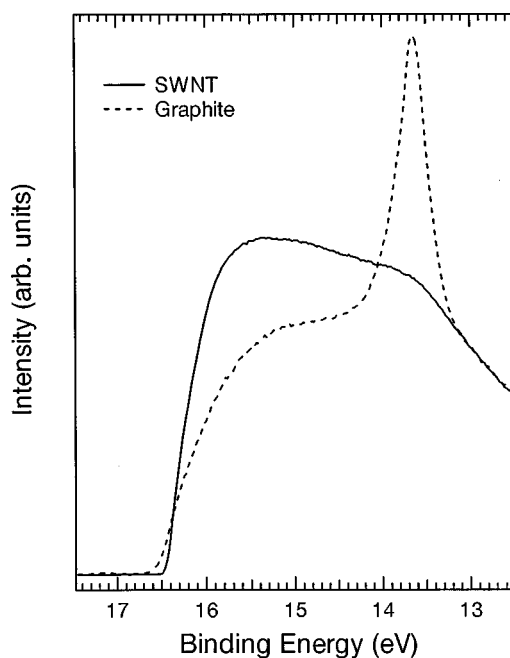


FIG. 3. Photoemission spectra around the secondary electron threshold regions of the pristine SWNT bundles and graphite.

the Cs intercalation is shown in Fig. 2. The peak grown with the Cs deposition is due to the Cs  $5p_{3/2}$ . From the relative intensity of the peak, the Cs/C compositional ratio at the deposition time of 30 min was estimated to be of the order of 0.1, by referring to a previous photoemission report<sup>14</sup> on Cs-intercalated graphite. In the figure, one can see a shift toward the higher binding energy side of the shoulder structures at 3 and 8.4 eV in pristine SWNTs. This indicates an upward shift of the Fermi level because of the electron transfer from Cs to C. The energy splitting of the two shoulder structures remained almost constant within the experimental error, indicating that the observed energy shifts can basically be described in terms of the rigid band shift. The binding energy shifts are about 0.25, 0.4, and 0.55 eV, respectively, for the deposition times of 5, 15, and 30 min. Thus, at first, the Fermi level rapidly shifted with the increase of the Cs concentration, and then, the movement gradually slowed. This can be ascribed to an increase of the density of states at the Fermi level caused by the intercalation.

Figure 3 shows the spectra around the secondary electrons threshold regions of the pristine SWNTs and graphite. The prominent peak of graphite at the nominal binding energy of about 13.6 eV is due to a large density of states in the unoccupied states,<sup>13</sup> and was assigned to the interlayer band that has large charge densities between carbon planes.<sup>15</sup> The corresponding peak almost disappears in the SWNT spectrum. This is quite reasonable because of the lack of the two-dimensional interlayers in a SWNT bundle.

As clearly seen in the figure, the threshold energy of the SWNT sample shifted by 0.1–0.2 eV to the lower binding energy side. This means that the SWNTs have a slightly larger work function than graphite. The increase of the work function in the SWNTs is completely opposite from the recent UPS results<sup>6,7</sup> on the MWNTs, in which work function decreases by 0.1–0.2 eV relative to graphite were observed. Furthermore, the actual values of the work functions ob-

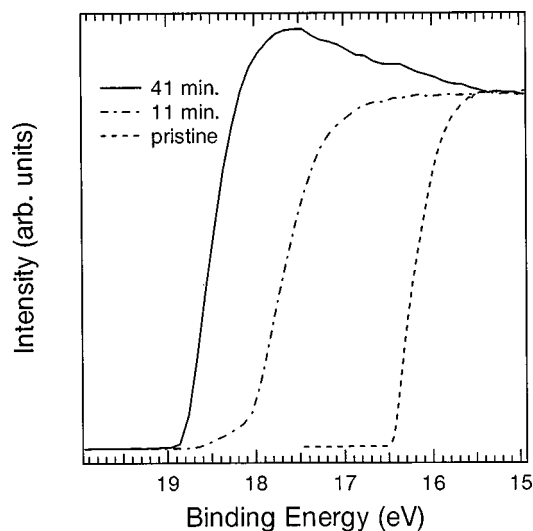


FIG. 4. Photoemission spectra around the secondary electron threshold regions of the pristine and the Cs-intercalated SWNT bundles for various Cs deposition times.

tained in this study are different from those of the previous reports. The work functions of the SWNT sample and graphite were determined to be about 4.8 and 4.6–4.7 eV, respectively, from the spectra in Fig. 3. The value for graphite determined in this study is fairly consistent with previous reports (4.6 eV).<sup>13,15</sup> On the other hand, Chen *et al.*<sup>6</sup> (estimated from the spectra in Ref. 6) and Ago *et al.*<sup>7</sup> gave values of about 5.7 and 4.3 eV for MWNTs, and 5.8 and 4.4 eV for graphite. It is unlikely that the relatively large work function value of the SWNTs is due to oxidation of the nanotubes<sup>7</sup> because we did not observe any prominent oxidized component in C 1s x-ray photoelectron spectrum. The effect of surface contamination can also be excluded because the sample was annealed before the measurement, as previously stated. The precise reason for the discrepancies is not clear. However, we stress that our experiment gives precisely the actual value of the work function of graphite, as mentioned above.

It is uncertain whether the work function of the SWNTs can be directly linked to their field emission properties at the present stage. It should be noted that the work function of a nanotube could be different at the tip and the side. It is considered that electrons are emitted from the nanotube tips rather than the sides even in the case of unaligned nanotube film.<sup>3</sup> On the other hand, the spectra measured in this study (as well as in Refs. 6 and 7) seem to be dominated by the contribution from the tube sides, because the nanotubes of the sample were not aligned.

Interestingly, the work function of the SWNT sample drastically decreased when Cs was deposited on the sample, as shown in Fig. 4. The threshold energies after Cs depositions (another run) of 11 and 41 min moved to the higher binding energy side by 1.7 and 2.4 eV, resulting in the work

functions of 3.1 and 2.4 eV, respectively. The reduction may be partly due to Cs atoms remaining on the bundle surface, which will induce an electric dipole moment at the surface due to the electron transfer. However, half a day after the Cs deposition, the degraded surface of the intercalated sample (prominent contaminant peaks were observed at about 5.7 and 9.7 eV) also showed a small work function of 2.55 eV, which is close to the value for the 41 min deposited sample. This suggests that the reduction is associated with the bulk property of the Cs-intercalated SWNTs. These results indicate that it would be interesting to measure the field emission properties of Cs-deposited carbon nanotubes.

In summary, the electronic structures of pristine and Cs-intercalated SWNT bundles were investigated using photoemission spectroscopy. The valence band states of the SWNTs were significantly different from that of graphite. Rigid band shift behavior was observed in the valence band states of the Cs-intercalated SWNT bundles. The work function of the pristine SWNTs was 0.1 to 0.2 eV larger than that of graphite, and it drastically decreased with the Cs deposition. The result suggests that Cs-intercalated SWNTs should have a lower electron emission threshold field than that of the pristine material.

S.S. is grateful to Dr. F. Maeda and Dr. S. Okada for their valuable discussions. Work done at UNC was supported by the Office of Naval Research through a MURI program (N00014-98-1-0597) and by a NASA graduate fellowship for C.B.

- <sup>1</sup>W. A. de Heer, A. Chatelain, and D. Ugarte, *Science* **270**, 1179 (1995).
- <sup>2</sup>Y. Saito, S. Uemura, and K. Hamaguchi, *Jpn. J. Appl. Phys., Part 2* **L346–348**, 37 (1998).
- <sup>3</sup>W. Zhu, C. Bower, O. Zhou, G. Kochanski, and S. Jin, *Appl. Phys. Lett.* **75**, 873 (1999).
- <sup>4</sup>R. H. Fowler and L. W. Nordheim, *Proc. R. Soc. London, Ser. A* **119**, 173 (1928).
- <sup>5</sup>P. G. Collins and A. Zettl, *Phys. Rev. B* **55**, 9391 (1997).
- <sup>6</sup>P. Chen, X. Wu, X. Sun, J. Lin, W. Ji and K. L. Tan, *Phys. Rev. Lett.* **82**, 2548 (1999).
- <sup>7</sup>H. Ago, T. Kugler, F. Cacialli, W. R. Salaneck, M. S. P. Shaffer, A. H. Windle, and R. H. Friend, *J. Phys. Chem. B* **103**, 8116 (1999).
- <sup>8</sup>C. Bower, S. Suzuki, K. Tanigaki, and O. Zhou, *Appl. Phys. A* **67**, 47 (1998).
- <sup>9</sup>C. Bower, O. Zhou, W. Zhu, A. G. Ramirez, G. P. Kochanski, and S. Jin, in *Amorphous and Nano-Structured Carbon*, edited by J. Robertson, J. Sullivan, O. Zhou, B. Coll, and T. Allen (Materials Research Society, Pittsburgh, in press).
- <sup>10</sup>T. Yildirim, O. Zhou, and J. E. Fischer, in *The Physics of Fullerene-Based and Fullerene-Related Materials*, edited by W. Andreoni (Kluwer, Dordrecht, in press).
- <sup>11</sup>X. P. Tang, A. Kleinhammes, H. Shimoda, L. Fleming, K. Y. Bennoune, S. Sinha, C. Bower, O. Zhou, and Y. Wu, *Science* **288**, 492 (2000).
- <sup>12</sup>S. Suzuki, C. Bower, and O. Zhou, *Chem. Phys. Lett.* **285**, 230 (1998).
- <sup>13</sup>D. Marchand, C. Fretigny, M. Lagues, F. Batallan, Ch. Simon, I. Rosenman, and R. Pinchaux, *Phys. Rev. B* **30**, 4788 (1984).
- <sup>14</sup>A. Fretigny, D. Marchand, and M. Lagues, *Phys. Rev. B* **82**, 8462 (1985).
- <sup>15</sup>F. Maeda, T. Takahashi, H. Ohsawa, S. Suzuki, and H. Suematsu, *Phys. Rev. B* **37**, 4482 (1988).